Cancer Cell
Article

Self-Renewal Does Not Predict Tumor Growth Potential in Mouse Models of High-Grade Glioma

Lindy E. Barrett,[1] Zvi Granot,[1] Courtney Coker,[1] Antonio Iavarone,[2] Dolores Hambardzumyan,[3] Eric C. Holland,[1] Hyung-song Nam,[1,4] and Robert Benezra[1,*]
[1]Department of Cancer Biology and Genetics, Memorial Sloan-Kettering Cancer Center, New York, NY 10021, USA
[2]Institute for Cancer Genetics, Department of Neurology, Columbia University Medical Center, New York, NY 10032, USA
[3]Department of Stem Cell Biology and Regenerative Medicine, Cleveland Clinic, Cleveland, OH 44195, USA
[4]Present address: Howard Hughes Medical Institute and Department of Human Genetics, University of Utah School of Medicine, Salt Lake City, UT 84112, USA
*Correspondence: r-benezra@ski.mskcc.org
DOI 10.1016/j.ccr.2011.11.025

SUMMARY

Within high-grade gliomas, the precise identities and functional roles of stem-like cells remain unclear. In the normal neurogenic niche, *ID* (*Inhibitor of DNA-binding*) genes maintain self-renewal and multipotency of adult neural stem cells. Using PDGF- and KRAS-driven murine models of gliomagenesis, we show that high Id1 expression (Id1^{high}) identifies tumor cells with high self-renewal capacity, while low Id1 expression (Id1^{low}) identifies tumor cells with proliferative potential but limited self-renewal capacity. Surprisingly, Id1^{low} cells generate tumors more rapidly and with higher penetrance than Id1^{high} cells. Further, eliminating tumor cell self-renewal through deletion of Id1 has modest effects on animal survival, while knockdown of Olig2 within Id1^{low} cells has a significant survival benefit, underscoring the importance of non-self-renewing lineages in disease progression.

INTRODUCTION

High-grade gliomas (WHO Grade III, IV astrocytomas) are among the most lethal types of solid tumors, with significant cellular and genetic heterogeneity complicating treatment efforts (Terzis et al., 2006). Since the discovery of glioma cells with properties reminiscent of neural stem cells, including the capacity to self-renew, there has been a great deal of interest in elucidating their contributions to tumorigenesis. Self-renewal in normal and tumor stem cells occurs when a cell divides to produce at least one daughter cell with the same developmental potential as itself, thus maintaining multipotency (He et al., 2009). This is in contrast to proliferation, which refers to cell divisions regardless of developmental potential (He et al., 2009). Within the subventricular zone (SVZ), normal adult neural stem cells (also referred to as "type B cells") are rare, slow-cycling and self-renewing cells that give rise to more rapid cycling transit amplifying cells ("type C cells"), which then give rise to more differentiated neuroblasts ("type A cells") (Doetsch et al., 1997). Glioma stem cells, likened to type B cells, are defined by their capacity to (1) self-renew in vitro, (2) transplant tumors in vivo, and (3) generate tumors that recapitulate the heterogeneity of the parental tumors (Stiles and Rowitch, 2008). The degree to which glioma stem cells resemble neural stem cells, and the degree to which the normal lineage hierarchy is maintained in brain tumors remain unanswered questions.

The cancer stem cell hypothesis predicts that stem cells are responsible for tumor initiation and preferentially drive tumor growth, and indeed, many studies use the term "glioma-initiating cell" (GIC) interchangeably with "glioma-stem cell" (GSC). However, whether stem-like cells are uniquely qualified in their ability to transplant disease, or whether other, more differentiated,

Significance

High-grade gliomas are typified by poor therapeutic response and rapid lethality. Using two mouse models of gliomagenesis, we identify and isolate two distinct stem- and progenitor-like tumor cell populations using a single marker, Id1. Id1^{high} glioma cells self-renew, giving rise to consistent proportions of differentiated lineages, while Id1^{low} cells have limited self-renewal capacity but retain proliferative potential. Although both populations transplant disease, Id1^{low} cells are more tumorigenic compared to Id1^{high} cells. Further, inhibiting the bHLH transcription factor Olig2 within Id1^{low} cells significantly prolongs the survival of tumor-bearing mice, while eliminating self-renewal of Id1^{high} cells has modest effects. These results have important implications for therapeutic strategies that seek to target stem- or progenitor- like cells within different subclasses of high-grade gliomas.

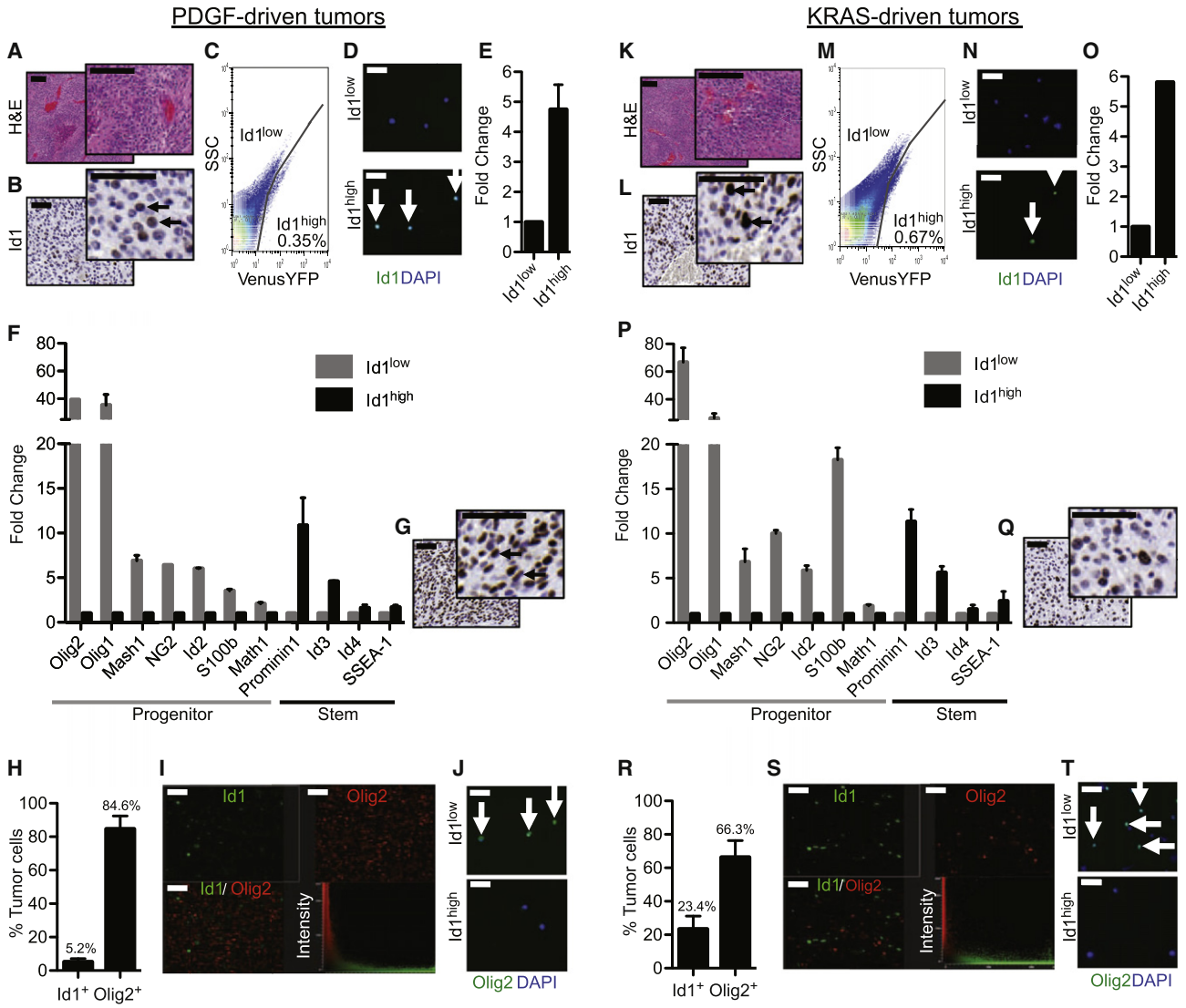

Figure 1. Tumors Can Be Separated into Id1^{high} and Id1^{low} Cell Populations

(A) Tumors were initiated with RCAS-PDGFB in Nestin-tva; Arf$^{-/-}$ mice (A–J). Staining with hematoxylin and eosin (H&E) shows high-grade features. Scale bars = 100 μm.

(B) Immunohistochemistry for Id1 reveals Id1+ cells within the tumor (arrows). Scale bars = 50 μm.

(C) FACS plot from Nestin-tva;Arf$^{-/-}$;Id1^{VenusYFP} tumors. Gray line indicates gate for VenusYFP signal.

(D) Id1 immunostaining on sorted Id1^{low} (top) and Id1^{high} (bottom) cells reveals Id1 expression restricted to the Id1^{high} cell population (arrows). Cells were counterstained with DAPI. Scale bars = 50 μm.

(E) Quantitative RT-PCR reveals enhanced Id1 expression in Id1^{high} compared to Id1^{low} cells.

(F) Quantitative RT-PCR for Olig2, Olig1, Mash1, NG2, Id2, S100b, Math1, Prominin1, Id3, Id4, SSEA-1 from Id1^{low} (gray bars) and Id1^{high} (black bars) sorted cells.

(G) Immunohistochemistry for Olig2 reveals a frequent expression pattern of Olig2+ cells (arrows). Scale bars = 50 μm.

(H) Graph shows percentage of Id1+ and Olig2+ tumor cells from PDGF-driven tumors.

(I) Immunostaining for Id1 (green), Olig2 (red) and spectral analysis showing intensity in red channel and green channels. Scale bars = 50 μm.

(J) Olig2 immunostaining on sorted Id1^{low} (top) and Id1^{high} (bottom) cells reveals Olig2 expression restricted to the Id1^{low} cell population (arrows). Cells were counterstained with DAPI. Scale bars = 50 μm.

(K) Tumors were initiated with RCAS-KRAS in Nestin-tva; Arf$^{-/-}$ mice (K-T). Staining with H&E shows high-grade features. Scale bars = 100 μm.

(L) Immunohistochemistry for Id1 reveals Id1+ cells within the tumor (arrows). Scale bars = 50 μm.

(M) FACS plot from Nestin-tva;Arf$^{-/-}$;Id1^{VenusYFP} tumors. Gray line indicates gate for VenusYFP signal.

(N) Id1 immunostaining on sorted Id1^{low} (top) and Id1^{high} (bottom) cells reveals Id1 expression restricted to the Id1^{high} cell population (arrows). Cells were counterstained with DAPI. Scale bars = 50 μm.

(O) Quantitative RT-PCR reveals enhanced Id1 expression in Id1^{high} compared to Id1^{low} cells.

(P) Quantitative RT-PCR for Olig2, Olig1, Mash1, NG2, Id2, S100b, Math1, Prominin1, Id3, Id4, SSEA-1 from Id1^{low} (gray bars) and Id1^{high} (black bars) sorted cells.

(Q) Immunohistochemistry for Olig2 reveals a frequent expression pattern of Olig2+ cells (arrows). Scale bars = 50 μm.

(R) Graph shows percentage of Id1+ and Olig2+ tumor cells from KRAS-driven tumors.

non-self-renewing lineages possess this capacity, remains controversial (Alcantara Llaguno et al., 2009; Chow et al., 2011; Lindberg et al., 2009; Prestegarden and Enger, 2010; Stiles and Rowitch, 2008). In other types of brain tumors, including medulloblastoma (Yang et al., 2008) and oligodendroglioma (Persson et al., 2010), cell lineages that express progenitor markers but are incapable of self-renewal in vitro have been shown to transplant disease. Further, oligodendrocyte precursor cells (OPCs) were recently identified as likely cells-of-origin in a p53/Nf1 mouse model of gliomagenesis, as lineage-analysis revealed this population to have the most dramatic growth expansion prior to malignancy (Liu et al., 2011). Adding to the complexity, it has been hypothesized that more differentiated cells may dedifferentiate and acquire a stem cell phenotype during the course of tumorigenesis (Kang et al., 2006). How frequently this occurs in vivo and whether the acquisition of self-renewal and "stemness" is a requisite for tumorigenic potential requires further investigation.

Critical to the analysis of high-grade gliomas is the identification of markers to definitively isolate and functionally characterize the distinct lineages. CD133 (Prominin-1) is the most common antigen used to identify glioma stem cells, but studies have shown that both $CD133^+$ and $CD133^-$ cells can self-renew and generate histologically distinct tumors (Beier et al., 2007; Chen et al., 2010; Clément et al., 2009; Wang et al., 2008), arguing against CD133 as a specific marker of glioma stem cells. Other studies have used the side population (SP) to define the stem-cell fraction, although this also identifies a heterogeneous population of both self-renewing and non self-renewing lineages (Broadley et al., 2011). The *ID (Inhibitor of DNA-binding)* genes are dominant negative regulators of basic helix-loop-helix transcription factors (Perk et al., 2005) with established roles in embryonic stem cell self-renewal (Romero-Lanman et al., 2011; Ying et al., 2003). Following development, Id1 continues to regulate self-renewal and differentiation in multiple somatic stem cell populations, including adult neural stem cells. High levels of Id1 identify type B adult neural stem cells within neurogenic niches, and Id1 and Id3 are required to maintain the self-renewal capacity of this cell population (Nam and Benezra, 2009). During lineage commitment, Id1 protein levels decrease as progenitor markers become more highly expressed (Nam and Benezra, 2009). While Id1 expression is low to absent in nonneurogenic regions of the normal adult brain, Id1 expression is upregulated in multiple subtypes of human and mouse gliomas (Anido et al., 2010; Vandeputte et al., 2002). Because high levels of Id1 identify self-renewing type B cells in the normal neurogenic niche, we hypothesized that high levels of Id1 could similarly identify glioma cells with a stem-cell phenotype.

Large-scale sequencing projects have identified alterations that frequently occur in human high-grade gliomas, including *PDGFRA* amplification (13%), alterations in RTK/RAS/PI(3)K signaling (88%) and *CDKN2A/Arf* homozygous deletion or mutation (49%) (Network, 2008). This has led to the generation of subclasses based upon specific genomic and proteomic signatures (Brennan et al., 2009; Huse et al., 2011; Network, 2008). Although studies differ with regard to subclass identity and nomenclature, broadly speaking, tumors with aberrant PDGFR signaling have been grouped in the Proneural subclass, and tumors with mutation and/or deletion of *NF1* have been grouped in the Mesenchymal subclass. The PDGFR/Proneural subclass has a well-established RCAS/tva-based mouse model, where adult *Nestin-tva;Arf*$^{-/-}$ mice are stereotaxically injected with RCAS-PDGFB into the SVZ, generating gliomas with near complete penetrance (Hambardzumyan et al., 2009, 2011). Tumors can also be initiated using constitutively active mutant KRAS, as KRAS has been shown to cooperate with tumor suppressor loss to generate gliomas (Uhrbom and Holland, 2001; Uhrbom et al., 2005). Tumors driven by either PDGF or KRAS show a histopathology that closely mimics human tumors, as well as high-grade features, including pseudopalisading necrosis and microvascular proliferation (Hambardzumyan et al., 2009, 2011; Uhrbom and Holland, 2001; Uhrbom et al., 2005).

Here, we test a central tenet of the cancer stem cell hypothesis, that self-renewal capacity is required for disease transplantation and is a key predictor of tumor growth potential, in PDGF- and KRAS-driven murine glioma models.

RESULTS

PDGF- and KRAS-Driven Tumors Can Be Separated into $Id1^{high}$ and $Id1^{low}$ Cell Populations

As shown in Figures 1A and 1B, tumors initiated with PDGF displayed high-grade features and upregulated Id1 expression, similar to what is observed in human high-grade gliomas (Figures S1A and S1B available online). In order to isolate and further characterize live tumor cells with high Id1 expression, we generated *Nestin-tva;Arf*$^{-/-}$*;Id1*^{VenusYFP} mice, where endogenous Id1 is fused to fluorescent VenusYFP and faithfully reports endogenous Id1 protein levels (Nam and Benezra, 2009). Following initiation with PDGF, tumors were dissociated and sorted based on VenusYFP expression into cell populations with high levels of VenusYFP (further referred to as $Id1^{high}$) and cell populations with undetectable levels of VenusYFP (further referred to as $Id1^{low}$) (Figure 1C). Post-sort analysis was used to confirm the absence of VenusYFP signal in the $Id1^{low}$ fraction (Figure S1C) and $Id1^{high}$ cells were, on average, 0.35% of the total sorted population, including stromal cells (Figure 1C). Immunostaining (Figure 1D) and RT-PCR (Figure 1E) confirmed Id1 expression in freshly sorted $Id1^{high}$ cells and low to undetectable levels of Id1 expression in freshly sorted $Id1^{low}$ cells. The stem-associated markers Prominin-1 and Id3 were more highly expressed in $Id1^{high}$ cells compared to $Id1^{low}$ cells (Figure 1F). In contrast, multiple progenitor-associated markers, including Olig2, Mash1, NG2, and Id2 were more highly expressed in $Id1^{low}$ cells compared to $Id1^{high}$ cells (Figure 1F).

Olig2 is known to regulate proliferation in neural progenitors (Ligon et al., 2007; Sun et al., 2011) and is expressed in multiple lineages, including type C cells in the normal neurogenic niche

(S) Immunostaining for Id1 (green), Olig2 (red) and spectral analysis showing intensity in red channel and green channels. Scale bars = 50 μm.
(T) Olig2 immunostaining on sorted $Id1^{low}$ (top) and $Id1^{high}$ (bottom) cells reveals Olig2 expression restricted to the $Id1^{low}$ cell population (arrows). Cells were counterstained with DAPI. Scale bars = 50 μm.
Error bars represent mean ± SD. See also Figure S1.

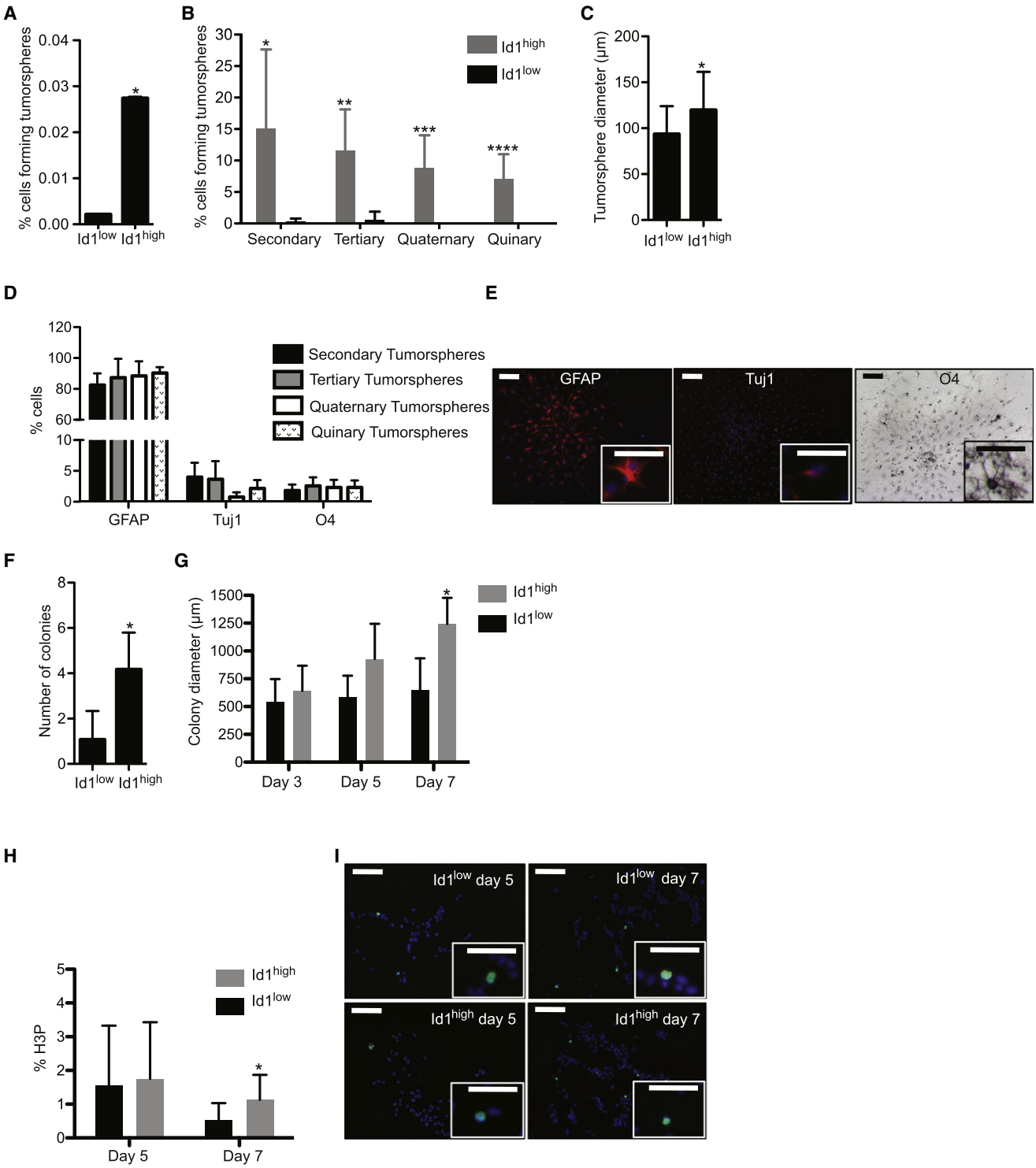

Figure 2. Id1^{high} Cells Are Characterized by High Self-Renewal Capacity, while Id1^{low} Cells Are Characterized By Limited Self-Renewal Capacity

(A) Percentage of sorted Id1^{high} and Id1^{low} cells forming primary tumorspheres from PDGF-driven tumors (10 cells/μl; *p = 2.37 × 10^{-7}).

(B) Percentage of sorted Id1^{high} (gray bars) and Id1^{low} (black bars) cells forming secondary, tertiary, quaternary and quinary tumorspheres from PDGF-driven tumors (1 cell/well; *p = 0.026, **p = 0.0084, ***p = 0.01, ****p = 0.007).

(C) Tumorsphere diameter was measured after 7 days in vitro for Id1^{low} (n = 60) and Id1^{high} (n = 128) tumorspheres (*p = 1.66 × 10^{-5}) from PDGF-driven tumors.

(D) Id1^{high} cells were used to generate secondary, tertiary, quaternary and quinary tumorspheres, which were then differentiated and the percentage of cells from individual tumorspheres that expressed GFAP, Tuj1, and O4 were quantified.

and mature oligodendrocytes (Menn et al., 2006). Olig2 is also expressed in all subtypes of malignant glioma (Ligon et al., 2004), leading us to more closely examine Olig2 expression in our model. Within PDGF-driven tumors, we observed high levels of Olig2 expression (Figure 1G), consistent with what is observed in human gliomas (Figures S1D and S1E) including those from the PDGFR subclass (Verhaak et al., 2010). By IHC, 5.2% of tumor cells had detectable levels of Id1 expression and 84.6% of cells had detectable levels of Olig2 expression (Figure 1H). Sorted Id1^{high} cells make up a subset of the total Id1-expressing population, as Id1 is expressed in varying levels in both tumor cells and stromal cells. Importantly, Olig2 and Id1 showed a largely mutually exclusive expression pattern (Figure 1I). Of Id1-expressing tumor cells, only 6.1% showed some level of Olig2 expression (Figure S1F). In the normal neurogenic niche, Id1 levels decrease and progenitor markers increase as cells transition from a type B cell to a type C cell phenotype (Nam and Benezra, 2009), and this population overlap within tumors may reflect a similar phenomenon. Importantly, we did not detect Olig2 protein expression in the sorted Id1^{high} population, and found significant Olig2 protein expression in the sorted Id1^{low} population (Figure 1J).

In order to test the generality of our results, we examined tumors driven by RCAS mutant KRAS using *Nestin-tva; Arf*$^{-/-}$*; Id1*^{VenusYFP} mice. As shown in Figures 1K and 1L, KRAS-driven tumors also displayed high-grade features and upregulated Id1 expression. By FACS, Id1^{high} cells represented, on average, 0.67% of the total sorted population including stromal cells (Figure 1M). Immunostaining (Figure 1N) and RT-PCR (Figure 1O) confirmed Id1 expression in freshly sorted Id1^{high} cells and low to undetectable levels of Id1 expression in freshly sorted Id1^{low} cells. Id1^{high} and Id1^{low} cells from KRAS-driven tumors showed a lineage-marker profile similar to what was observed from PDGF-driven tumors (Figure 1P). Compared to PDGF-driven tumors, KRAS-driven tumors had more Id1-expressing cells by IHC and fewer Olig2-expressing cells, with 23.4% of tumor cells expressing Id1 and 66.3% of tumor cells expressing Olig2 (Figures 1Q and 1R). Coimmunostaining for Id1 and Olig2 again revealed a largely mutually exclusive expression pattern (Figure 1S). Importantly, we did not detect Olig2 protein expression in the sorted Id1^{high} cells, and found significant Olig2 protein expression in the sorted Id1^{low} cells (Figure 1T). Thus, in both PDGF- and KRAS-driven tumors, sorted Id1^{high} cells were characterized by high levels of the neural stem cell marker Id1, and an absence of common progenitor-associated markers. While Id1^{low} cells represented heterogeneous tumor bulk, they were characterized by high levels of Olig2 and other progenitor-associated markers.

We further characterized the expression of Id1 and several lineage markers using human glioma tissue microarrays (TMAs). Here, we found that a subset of Id1-expressing cells also expressed the putative stem-cell marker CD133, although we observed both CD133^{+}/Id1^{-} and CD133^{-}/Id1^{+} cells (Figure S1G). While Id1 and Olig2 showed a largely exclusive expression pattern in the PDGF- and KRAS-driven murine models, we identified two distinct groups from the human TMAs: one group showed a largely exclusive expression pattern between Id1 and Olig2, while the other group showed a high-degree of overlap between the two proteins (Figures S1D and S1E). We speculate that differences may exist in the Id1/Olig2 lineage relationship, and expression of stem and progenitor cells generally, within distinct subtypes of high-grade gliomas.

Id1^{high} Tumor Cells Have Stem Cell Properties, while Id1^{low} Tumor Cells Resemble Progenitor Cells

We hypothesized that high levels of Id1 would identify tumor cells with a stem cell phenotype, similar to what is observed in type B cells of the normal neurogenic niche. To assess the self-renewal capacity of Id1^{high} and Id1^{low} glioma cells, we plated cells at clonal density in the presence of epidermal growth factor (EGF) and fibroblast growth factor (FGF) and characterized tumorsphere formation and colony formation in vitro. From PDGF-driven tumors, freshly sorted Id1^{high} cells showed a 12.8-fold enhancement in primary tumorsphere formation compared to Id1^{low} cells (Figure 2A; 10 cells/μl). Similar results were obtained when cells were plated to form tumorspheres prior to sorting to eliminate stroma and then dissociated, sorted into Id1^{high} and Id1^{low} populations and replated to form tumorspheres (Figure S2A; 10 cells/μl). Primary tumorspheres were dissociated and plated at clonal density (1 cell/well) over serial passages. From Id1^{high} primary tumorspheres, 15.06% of single cells formed secondary tumorspheres, of which 11.62% of single cells formed tertiary tumorspheres, 8.82% of single cells formed quaternary tumorspheres, and 7.10% of single cells formed quinary tumorspheres (Figure 2B). By contrast, from Id1^{low} primary tumorspheres, 0.33% of single cells formed secondary tumorspheres, of which 0.625% of single cells formed tertiary tumorspheres, with no generation of tumorspheres over additional passages (Figure 2B). Id1^{high} cells generated tumorspheres that were marginally larger than those generated from Id1^{low} cells (Figure 2C). Similar results were observed in KRAS-driven tumors, where Id1^{high} cells showed a 7.5-fold enhancement in primary tumorsphere formation compared to Id1^{low} cells (Figure S2B; 10 cells/μl). From Id1^{high} primary tumorspheres, 7.67% of cells formed secondary tumorspheres, 1.85% of cells formed tertiary tumorspheres, and 0.267% of cells formed quaternary tumorspheres (plated 0.5 cells/μl; Figure S2C). By contrast, we were unable to generate secondary tumorspheres

(E) Representative images of tumorspheres generated from Id1^{high} cells that were differentiated and stained for GFAP, Tuj1, and O4. Scale bars = 100 μm for main images, 50 μm for insets. Cells were counterstained with DAPI in fluorescent images.
(F) Number of adherent colonies formed after 7 days in vitro from Id1^{low} cells (n = 14) compared to Id1^{high} cells (n = 24) (0.5 cells/μl; *p = 5.29 × 10^{-7}).
(G) Diameter of adherent colonies measured after 3 days (p = 0.38; n = 17), 5 days (p = 0.04; n = 27) and 7 days (*p = 6.39 × 10^{-5}; n = 14) from Id1^{low} cells (black bars) compared to Id1^{high} cells (gray bars).
(H) Percentage of phosphohistone H3 expressing cells within adherent colonies from Id1^{low} cells (black bars) compared to Id1^{high} cells (gray bars) after 5 days (p = 0.75; n = 16) or 7 days (*p = 0.014; n = 35).
(I) Representative images of Id1^{low} and Id1^{high} adherent colonies after 5 or 7 days stained for H3P (green) and counterstained with DAPI. Scale bars = 100 μm for main images, 50 μm for insets.
Error bars represent mean ± SD. See also Figure S2.

from the Id1^{low} primary tumorspheres at this plating density (Figure S2C).

Id1^{low} secondary tumorspheres, as well as Id1^{high} secondary, tertiary, quaternary, and quinary tumorspheres from the PDGF-driven model were plated under conditions to favor differentiation, and the resultant progeny were quantified. While undifferentiated tumorspheres showed low to absent expression of GFAP, O4, and Tuj1 (Figures S2D and S2E), individual Id1^{high} secondary tumorspheres primarily generated GFAP-expressing astrocytes upon differentiation, with less frequent but consistent generation of O4-expressing oligodendrocytes and Tuj1-expressing neurons (Figures 2D and 2E; Figure S2F). Essentially all individual Id1^{high} tumorspheres showed similar percentages of cells expressing these markers. We also observed similar proportions of GFAP-, O4-, and Tuj1-expressing cells from Id1^{high} tumorspheres at tertiary, quaternary, and quinary passages (Figure 2D; Figure S2F), consistent with these populations undergoing self-renewal events, rather than physical events such as in vitro fusion. The fact that the Id1^{high} population primarily differentiated into GFAP-expressing cells is also consistent with studies showing a role for Id1 in restraining neural differentiation (Ying et al., 2003). Id1^{low} secondary tumorspheres, by contrast, showed a high degree of variability with regards to their differentiation potential: 37.5% primarily generated GFAP-expressing cells, 43.75% primarily generated Tuj1-expressing cells, and 18.75% generated roughly equal numbers of GFAP- and Tuj1-expressing cells (n = 16; Figure S2G). The generation of O4-expressing cells was sporadic, found within approximately 18% of differentiated Id1^{low} secondary tumorspheres (Figure S2G). Thus, Id1^{high} glioma cells displayed a classic stem-cell phenotype in vitro, while Id1^{low} glioma cells, depleted of stromal cells, were found to possess limited self-renewal capacity.

Id1^{low} and Id1^{high} cells derived from PDGF-driven tumors were also plated at clonal density (0.5 cells/μl) as adherent monolayers using the same mitogenic conditions as in the nonadherent tumorsphere assays. Id1^{high} cells generated colonies more frequently than Id1^{low} cells (Figure 2F), and generated colonies that were marginally larger than those generated from Id1^{low} cells (Figure 2G), paralleling our tumorsphere data (Figures 2A–2C). We did not observe significant differences in expression of cleaved caspase-3 between colonies generated from Id1^{low} and Id1^{high} cells (data not shown), nor did we observe differences in H3P expression after 5 days in vitro (Figures 2H and 2I). Id1^{high} colonies did show approximately 2-fold greater H3P expression at 7 days in vitro suggesting a modest proliferative advantage (Figures 2H and 2I). Nonetheless, both Id1^{low} and Id1^{high} cells were capable of proliferation, suggesting that the dramatic differences in tumorsphere formation between the Id1^{low} and Id1^{high} cell populations were due largely to differences in self-renewal capacity, as opposed to an inability of the Id1^{low} cells to proliferate under the conditions used in our assays.

Id1^{low} Cells More Efficiently Transplant Disease than Id1^{high} Cells

We next probed the capacity of Id1^{low} and Id1^{high} glioma cells to transplant disease by injecting 1.0 × 10^3 freshly sorted cells into the cortex of adult Nude/NCr host mice. From PDGF-driven tumors, both Id1^{low} and Id1^{high} cells were capable of generating high-grade gliomas (Figures 3A and 3B). However, Id1^{low} cells generated tumors more quickly and with higher penetrance: mice injected with 1.0 × 10^3 Id1^{low} cells had a median survival of 35.5 days compared to mice injected with 1.0 × 10^3 Id1^{high} cells, which had a median survival of 62 days (Figure 3A). Tumors were generated in 73.7% of mice injected with 1.0 × 10^3 Id1^{low} cells compared to 46.7% of mice injected with 1.0 × 10^3 Id1^{high} cells (Figure 3A). We were unable to generate tumors with 1.0 × 10^3 cells from either Id1^{low} or Id1^{high} cells when they were plated in vitro prior to transplantation (data not shown). Plating cells in vitro also led to changes in Id1 and Olig2 expression (Figures S3A–S3C), and we therefore injected freshly sorted cells in all experiments, allowing us to avoid in vitro selection bias and analyze the lineages in a minimally perturbed state. We also performed the same experiments using 1.0 × 10^3 Id1^{high} or Id1^{low} cells isolated from KRAS-driven tumors. Here, 52.6% of mice injected with 1.0 × 10^3 Id1^{low} cells developed high-grade tumors, with a median survival of 37 days (Figure 3C), while 1 of 19 mice (5.3%) injected with 1.0 × 10^3 Id1^{high} cells developed a low-grade tumor with a survival of 119 days (Figure 3C). Therefore, in both PDGF- and KRAS-driven tumors, Id1^{low} cells generated tumors more quickly and with higher penetrance than Id1^{high} cells.

Tumors initiated with either Id1^{low} or Id1^{high} cells expressed Nestin, GFAP, and Tuj1 (Figures S3D and S3E), although the majority of tumor cells expressed Olig2 (Figures 3B and 3D). The fact that Id1^{high} cells did not express Olig2 upon isolation indicates that Id1-expressing tumor cells were generating Olig2-expressing tumor cells in vivo. This is consistent with studies in the normal SVZ, which show that type B cells can generate oligodendrocyte lineages (Jackson et al., 2006; Menn et al., 2006), and with the observation that Id1^{high} B-type cells give rise to Id1^{low} (Mash1$^+$, Olig2$^+$) progenitor cells (Nam and Benezra, 2009). Surprisingly, both Id1^{low} and Id1^{high} cells generated tumors with Id1 expression (Figures 3B and 3D).

To determine the source of Id1 expression in tumors initiated with Id1^{low} cells, we injected 1.0 × 10^3 Id1^{low} cells from the PDGF-driven model into the cortex of *ubc-GFP;NOD-SCID* mice, which express GFP in all cells (Figure 4A). Immunostaining for Id1 revealed that Id1 expression was restricted to GFP expressing cells (Figure 4B). We did not observe Id1-expressing/GFP-nonexpressing cells (Figure 4C), indicating that the Id1 expressing cells were in fact host-derived. In contrast to Id1, immunostaining for Olig2 did not colocalize with GFP, indicating that the Olig2 expressing cells were coming from the initiating cell population (Figures 4D and 4E). We also observed recruitment using cells isolated from the KRAS-driven model (Figure S4A). These data are consistent with studies in other model systems showing that cells recruited from the normal brain parenchyma can contribute to glioma heterogeneity (Assanah et al., 2006). To determine whether Id1 expression in the recruited population was important for tumor growth, we injected 1.0 × 10^3 Id1^{low} cells from PDGF-driven tumors into the cortex of Id1$^{-/-}$ mice. These mice also developed tumors (Figure S4B), indicating that Id1 expression in the recruited cells was not essential for tumorigenic potential. Further, both Id1^{low} and Id1^{high} cells led to recruitment of similar numbers of cells (Figure S4C), suggesting that the differences in tumor initiation between Id1^{low} and Id1^{high} cells were not due to their relative capacity for recruitment. Most importantly, Id1^{low} cells were

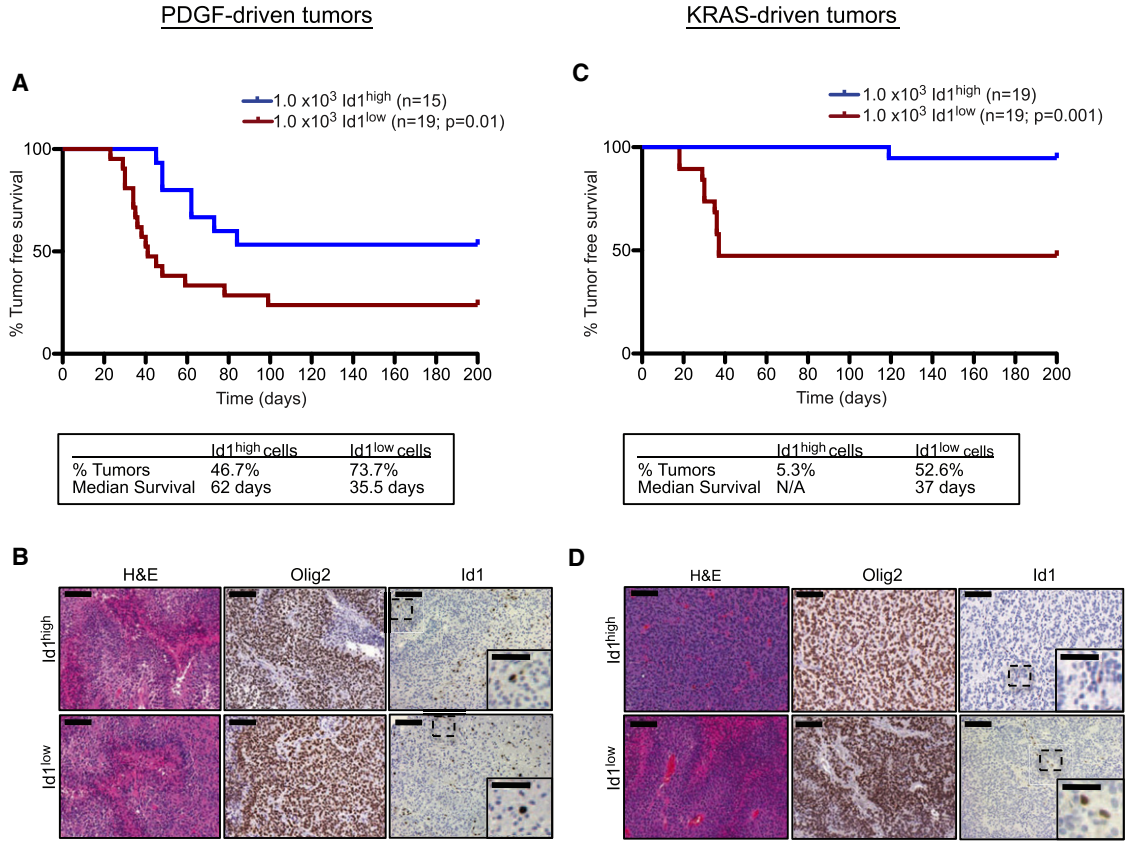

Figure 3. Id1^{low} Cells Transplant Disease More Efficiently than Id1^{high} Cells

(A) Kaplan-Meier analysis comparing mice injected with 1.0 × 10^3 Id1^{low} cells (n = 19; red line) or 1.0 × 10^3 Id1^{high} cells (n = 15; blue line) from PDGF-driven tumors. Chart shows percentage of mice that developed tumors and median survival.

(B) Representative images of H&E, Olig2 and Id1 immunohistochemistry for tumors generated with either Id1^{low} (bottom) or Id1^{high} (top) cells from PDGF-driven tumors. Scale bars = 100 μm for main images, 50 μm for insets.

(C) Kaplan-Meier analysis comparing mice injected with 1.0 × 10^3 Id1^{low} cells (n = 19; red line) or 1.0 × 10^3 Id1^{high} cells (n = 19; blue line) from KRAS-driven tumors. Chart shows percentage of mice that developed tumors and median survival.

(D) Representative images of H&E, Olig2 and Id1 immunohistochemistry for tumors generated with Id1^{low} (bottom) or Id1^{high} (top) cells from KRAS-driven tumors. Scale bars = 100 μm for main images, 50 μm for insets. See also Figure S3.

not reverting to an Id1-expressing state during the course of tumorigenesis and therefore this type of conversion could not explain the tumorigenic potential of the Id1^{low} cell population.

Inhibiting the Self-Renewal Capacity of Id1^{high} Cells Has Modest Effects on Tumor Growth

To determine how a reduction in self-renewal capacity would impact tumor growth, we generated *Nestin-tva;Arf*$^{-/-}$ mice with the following genotypes: *Id1*$^{+/+}$;*Id3*$^{+/+}$, *Id1*$^{-/-}$;*Id3*$^{+/+}$, and *Id1*$^{-/-}$;*Id3*$^{+/-}$. As shown in Figure 5, loss of Id1 led to dramatic reductions in tumor cell self-renewal capacity. *Id1*$^{-/-}$;*Id3*$^{+/+}$ and *Id1*$^{-/-}$;*Id3*$^{+/-}$ mice had a 5- to 10-fold reduction in primary tumorsphere formation compared to *Id1*$^{+/+}$;*Id3*$^{+/+}$ mice (Figure 5A; 10 cells/μl). From *Id1*$^{+/+}$;*Id3*$^{+/+}$ mice, 19.8% of cells formed secondary tumorspheres, compared to 0.067% of cells from *Id1*$^{-/-}$;*Id3*$^{+/+}$ mice and 0.21% of cells from *Id1*$^{-/-}$;*Id3*$^{+/-}$ mice (Figure 5B; 1 cell/well). *Id1*$^{+/+}$ *Id3*$^{+/+}$ tumorspheres primarily differentiated into GFAP-expressing cells, with less frequent but consistent generation of O4- and Tuj1-expressing cells (Figures 5C and 5D). We observed similar proportions of GFAP-, O4-, and Tuj1-expressing cells from secondary and tertiary tumorspheres (Figures 5C and 5D), and a pattern of differentiation closely paralleling that of Id1^{high} tumorspheres (Figures 2D and 2E).

Cells from *Id1*$^{+/+}$;*Id3*$^{+/+}$ and *Id1*$^{-/-}$;*Id3*$^{+/-}$ mice were also plated as adherent monolayers at clonal density (0.5 cells/μl). Cells plated from *Id1*$^{-/-}$;*Id3*$^{+/-}$ tumors generated fewer adherent colonies than cells plated from *Id1*$^{+/+}$;*Id3*$^{+/+}$ tumors (Figure 5E) and while the average H3P expression in *Id1*$^{-/-}$;*Id3*$^{+/-}$ colonies was slightly lower compared to *Id1*$^{+/+}$;*Id3*$^{+/+}$ colonies at 7 days in vitro, these differences were not statistically significant (Figure 5F). Thus, both cell populations were capable of proliferation in vitro.

The reduction in self-renewal capacity with Id loss mirrors the effects of Id loss in normal adult neural stem cells (Nam and Benezra, 2009). However, we observed only modest effects of Id loss on tumor-free survival (Figure 5G). Similar effects on tumor-free survival were observed following conditional loss of Id1 in *Nestin-tva;Arf*$^{-/-}$ mice: after coinjection of RCAS-PDGFB and RCAS-Cre, *Id1*$^{+/+}$;*Id3*$^{+/+}$ mice had a median survival of 28 days and *Id1*$^{flox/flox}$;*Id3*$^{+/+}$ mice had a median survival of

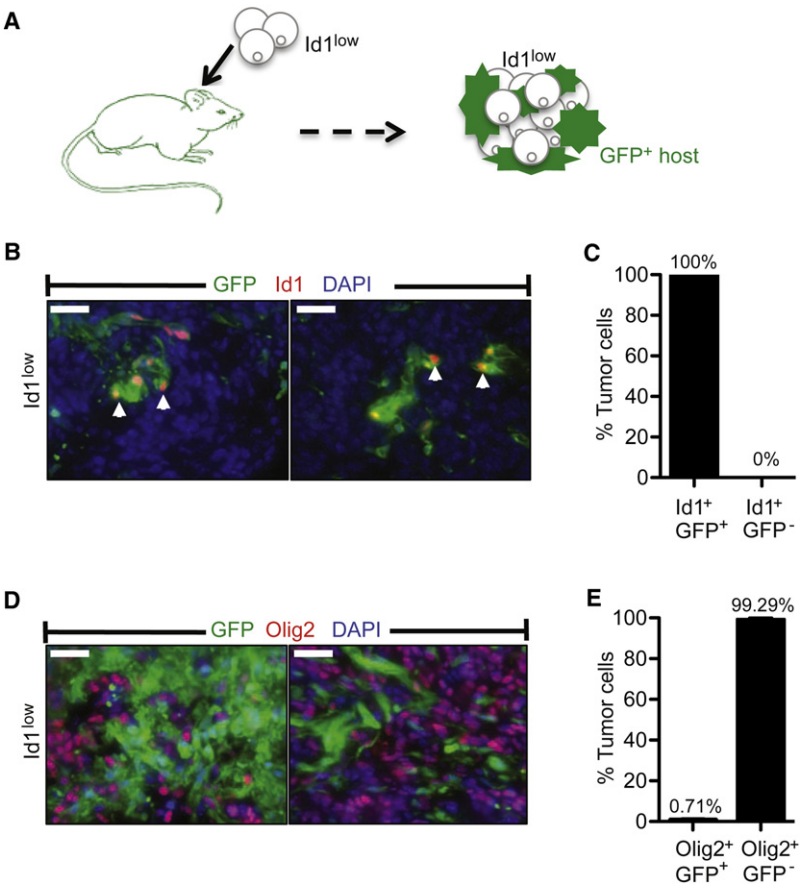

Figure 4. Id1^{low} Cells Do Not Revert to an Id1-Expressing State In Vivo

(A) Schematic illustrating the injection of Id1^{low} (nonfluorescent) cells into ubc-GFP;NOD-SCID host mice.

(B) Two representative images showing coimmunostaining for GFP and Id1. Note the presence of Id1^{+}/GFP^{+} cells (arrowheads). Tissue was counterstained with DAPI. Scale bars = 50 μm.

(C) Percentage of tumor cells that were Id1+/GFP+ compared to Id1^{+}/GFP^{-} (n = 4 mice, >900 Id1^{+} cells).

(D) Two representative images showing coimmunostaining for GFP and Olig2. Tissue was counterstained with DAPI. Scale bars = 50 μm.

(E) Percentage of tumor cells that were Olig2+/GFP+ compared to Olig2^{+}/GFP^{-} (n = 4 mice, >900 Olig2+ cells). Error bars represent mean ± SD. See also Figure S4.

34 days (Figure S5). In normal adult neural stem cells, Id1 and Id3 show redundancy of function at the level of self-renewal (Nam and Benezra, 2009). We therefore probed the effects of combined Id1 and Id3 loss to eliminated potential compensation between Id proteins. *Nestin-tva;Arf*$^{-/-}$ *Id1*$^{flox/flox}$*; Id3*$^{-/-}$ mice injected with RCAS-PDGFB and RCAS-Cre had a median survival no different from control animals (28 days; Figure S5).

Id1^{low} tumor cells showed significant growth potential in vivo (Figure 3), and we hypothesized that inhibiting the growth of the Id1^{low} population might confer a more significant survival benefit. As Olig2 is a known mediator of glioma growth in cell line models, we inserted an H1 promoter driving Olig2 shRNA downstream of PDGFB in the RCAS vector (Figures S6A and S6B). Using RCAS-PDGFB;Olig2-shRNA or RCAS-PDGFB; shRNA-Control constructs to initiate tumors, we found that Olig2 knockdown significantly increased tumor-free survival (Figure 6A). Olig2 knockdown was confirmed in tumors that were removed at early time points from presymptomatic mice (Figure 6B). Tumors that grew out from the Olig2 shRNA condition expressed Olig2 (Figure 6C), consistent with previous reports showing a significant role for Olig2 in human and mouse gliomas (Ligon et al., 2007; Mehta et al., 2011). To further explore the relationship between Id1 and Olig2, primary mouse glioma cells were transiently transfected with Id1 siRNA, Olig2 siRNA or Control siRNA. Knockdown of Id1 did not affect Olig2 expression levels, and knockdown of Olig2 did not affect Id1 expression levels (Figure S6C), suggesting that neither gene directly represses the other in our model system.

To begin to explore the role of Id1 and stem-like cells in human high-grade gliomas, we analyzed survival data from The Cancer Genome Atlas for each of the identified subtypes (Verhaak et al., 2010) based on Id1 expression for patients diagnosed with primary GBMs. Patients were subdivided into those with high Id1 expression (top 50%) and those with low Id1 expression (bottom 50%), compared to the unfiltered data set (Figures 7A–7D). Within the Proneural subclass, patients with high Id1 expression had a median survival of 22.015 months, compared to patients with low Id1 expression, which had a median survival of 6.015 months (Figure 7D). No significant differences in survival were observed for the Classical, Mesenchymal and Neural subtypes when subdivided by Id1 expression (Figures 7A–7C). As the PDGF-driven murine model most closely mimics the Proneural subclass, this human data, while correlative, is consistent with our finding that low Id1 expression identifies a more aggressive tumor cell population in this subtype.

DISCUSSION

Self-renewal is the defining characteristic of both normal and cancer stem cells. It has been postulated that glioma cells with stem cell properties preferentially transplant disease and contribute disproportionately to tumor growth compared to other, more differentiated lineages. Our results argue against this stringent interpretation of the cancer stem cell hypothesis. Using a marker of normal adult neural stem cells, we identified glioma cells with high self-renewal capacity and compared their tumorigenic potential to that of low self-renewing lineages. We found that in PDGF- and KRAS- driven mouse glioma models, both cell populations were capable of transplanting disease, and cells with low self-renewal capacity were actually more tumorigenic. Thus, GICs cannot be exclusively identified by self-renewal or "stemness."

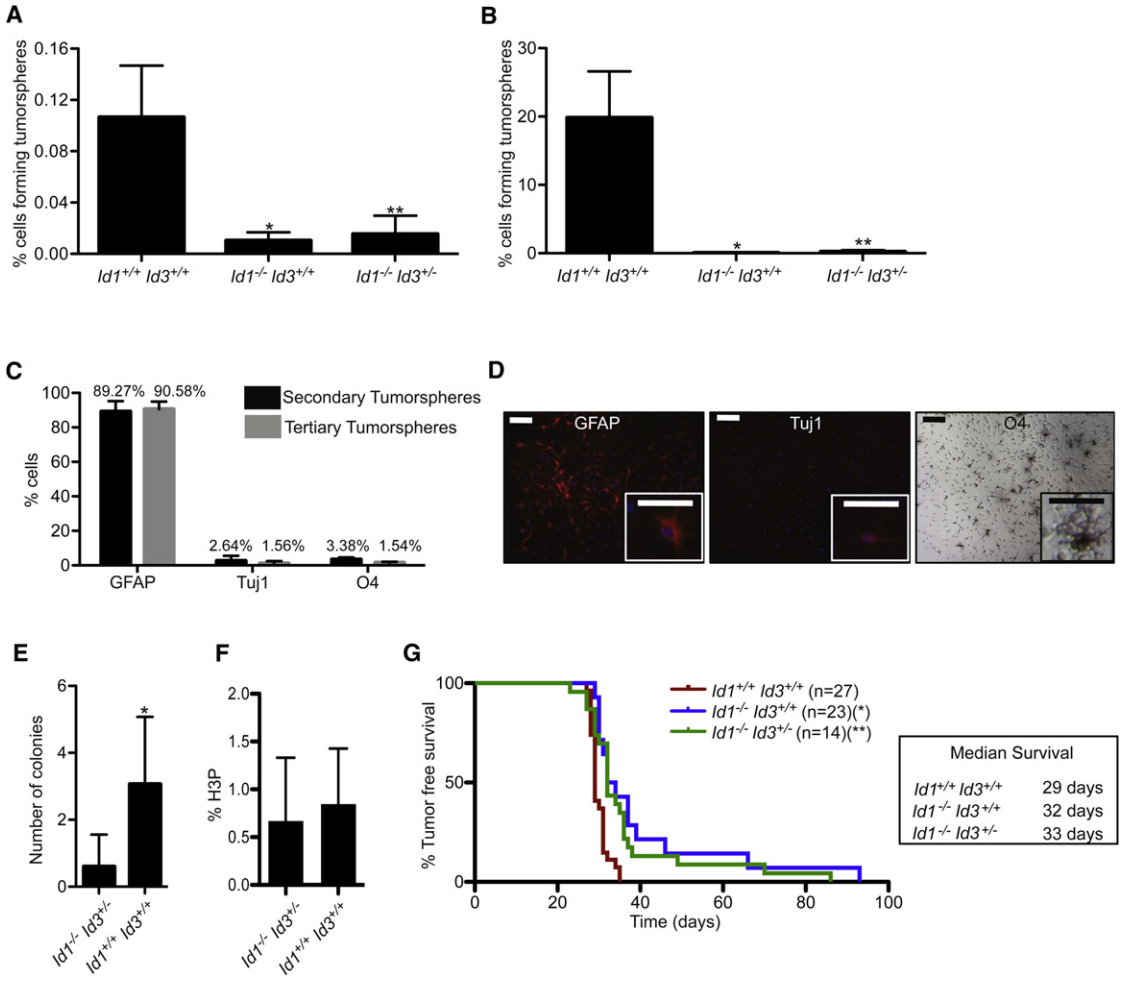

Figure 5. Id1-Loss Significantly Impacts Tumor Cell Self-Renewal but Has Only Modest Effects on Tumor-Free Survival

(A) Percentage of cells forming primary tumorspheres from PDGF-driven tumors (10 cells/μl) using *Nestin-tva;Arf*$^{-/-}$ *;Id1*$^{-/-}$*;Id3*$^{+/+}$ mice (n = 4; *p = 0.0017), *Nestin-tva;Arf*$^{-/-}$ *;Id1*$^{-/-}$*;Id3*$^{+/-}$ mice (n = 5; **p = 0.001) and *Nestin-tva;Arf*$^{-/-}$ *;Id1*$^{+/+}$*;Id3*$^{+/+}$ mice (n = 6).

(B) Percentage of cells forming secondary tumorspheres from PDGF-driven tumors (0.5 cells/μl) using *Nestin-tva;Arf*$^{-/-}$ *;Id1*$^{-/-}$*;Id3*$^{+/+}$ mice (n = 3; *p = 0.0044), *Nestin-tva;Arf*$^{-/-}$ *; Id1*$^{-/-}$*;Id3*$^{+/-}$ mice (n = 5; **p = 0.0003) and *Nestin-tva;Arf*$^{-/-}$ *;Id1*$^{+/+}$*;Id3*$^{+/+}$ mice (n = 4).

(C) Percentage of cells from secondary or tertiary tumorspheres that differentiated into GFAP, Tuj1, and O4 expressing cells. Tumorspheres were generated from *Nestin-tva;Arf*$^{-/-}$ *;Id1*$^{+/+}$*;Id3*$^{+/+}$ mice.

(D) Representative images of tumorspheres generated from *Id1*$^{+/+}$*;Id3*$^{+/+}$ cells, differentiated, and stained for GFAP, Tuj1, and O4. Scale bars = 100 μm for main images, 50 μm for insets. Cells were counterstained with DAPI in fluorescent images.

(E) Number of adherent colonies formed after 7 days in vitro from *Id1*$^{+/+}$*;Id3*$^{+/+}$ cells compared to *Id1*$^{-/-}$*;Id3*$^{+/-}$ cells (0.5 cells/μl; *p = 4.98 × 10^{-8}).

(F) Percentage of phosphohistone H3 (H3P) expressing cells within adherent colonies from *Id1*$^{+/+}$ *Id3*$^{+/+}$ compared to *Id1*$^{-/-}$ *Id3*$^{+/-}$ mice after 7 days in vitro (p = 0.44).

(G) Kaplan-Meier analysis comparing *Nestin-tva;Arf*$^{-/-}$ *;Id1*$^{+/+}$*;Id3*$^{+/+}$ mice (n = 27) with *Nestin-tva;Arf*$^{-/-}$ *;Id1*$^{-/-}$*;Id3*$^{+/+}$ mice (n = 23; *p = 0.0003) and *Nestin-tva;Arf*$^{-/-}$ *;Id1*$^{-/-}$*;Id3*$^{+/-}$ mice (n = 14; **p = 0.0003). Tumors were initiated with PDGF. Chart shows median survival.

Error bars represent mean ± SD. See also Figure S5.

Using Id1 to Identify Stem-Like Glioma Cells

Unlike the clearly defined, marker restricted lineages that exist in the hematopoietic system, stem and progenitor cells in the normal neurogenic niche and in brain tumors remain relatively ill-defined, complicating efforts to assign functional roles to these cell populations. While many studies use CD133 (Prominin 1) to identify glioma stem cells, CD133^{-} cells can also self-renew, suggesting that CD133 expression alone does not definitively identify glioma stem cells. High Id1 expression identifies type B cells in the normal neurogenic niche, and Id1 levels decrease gradually during lineage commitment (Nam and Benezra, 2009). Reversion from an Id1^{low} to an Id1^{high} state is never observed, and we have therefore taken advantage of the Id1-VenusYFP knockin strain to isolate cells with high levels of Id1 within murine gliomas, and specifically identify the stem-like fraction.

We define self-renewal capacity by the ability of cells to form multipotent tumorspheres of consistent progeny over serial passages when plated at clonal density in serum-free, adherent-free conditions. While definitive assays for self-renewal remain

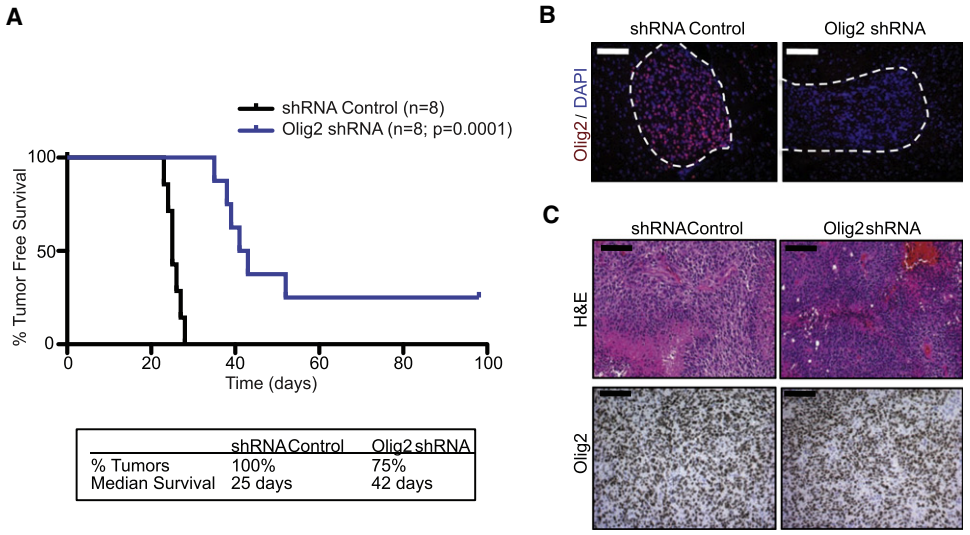

Figure 6. Targeting Id1^{low} Progenitor-Like Cells via Knockdown of Olig2 Shows a Significant Survival Benefit

(A) Kaplan-Meier analysis comparing *Nestin-tva;Arf*$^{-/-}$ mice injected with RCAS-PDGFB-shRNA Control or RCAS-PDGFB-Olig2 shRNA. Chart shows percentage of mice that developed tumors and median survival.

(B) Olig2 immunostaining from tumors (dotted line) generated with shRNA Control or Olig2 shRNA. Tumors were analyzed from pre-symptomatic mice. Tissue was counterstained with DAPI. Scale bars = 100 μm.

(C) H&E and Olig2 immunohistochemistry from tumors generated with shRNA Control or Olig2 shRNA. Tumors were analyzed when mice became symptomatic. Scale bars = 100 μm. See also Figure S6.

a matter of controversy, the ability of a glioma cell to form a tumorsphere under defined conditions has historically been used as an in vitro measure of self-renewal (Galli et al., 2004; Pastrana et al., 2011; Singh et al., 2003, 2004). A recent review by Pastrana et al. (2011) highlights a number of important considerations for the design and interpretation of sphere-formation assays. Importantly, we sorted fluorescent cells directly from transgenic mice, eliminating issues related to antibody labeling and antigen presentation. We also plated cells in identical mitogenic conditions and used clonal densities to reduce the likelihood of aggregations. Further, we confirmed the multipotency and proliferation potential of our cell populations. Under these experimental conditions, Id1^{high} glioma cells were characterized by high self-renewal capacity, giving rise to tumorspheres with similar proportions of differentiated progeny over multiple passages, and thus maintaining multipotency. Id1^{high} cells also gave rise to heterogeneous tumors in vivo, fulfilling the criteria of glioma stem cells. By contrast, Id1^{low} glioma cells were characterized by low self-renewal capacity, generating tumorspheres with variable proportions of differentiated progeny. Undifferentiated Id1^{low} cells also expressed progenitor markers (including high levels of Olig2), and had the ability to generate heterogeneous tumors in vivo, making them more characteristic of multipotent progenitors. It has been hypothesized that, within tumors, Olig2 may represent a transition from a type B cell to a type C cell, although Olig2 is also expressed in more differentiated lineages (Ligon et al., 2007). Taken together, our data suggest that Id1^{high} glioma cells resemble type B cells, at or near the top of the lineage hierarchy, while Id1^{low} cells more closely resemble type C cells.

Tumor Cell Self-Renewal Does Not Predict Tumor Growth Potential

Our data show that Id1^{low} glioma cells resembling type C cells have greater tumorigenic potential than Id1^{high} glioma cells reminiscent of type B cells in PDGF- and KRAS-driven tumors (Figure 8). Although it is important to note that both populations were capable of transplanting disease, we were surprised to find that Id1^{low} cells generated tumors more quickly and with higher penetrance, indicating that self-renewal did not cosegregate with tumorigenic potential. Thus, the ability of a glioma cell to proliferate even while changing state (as seen in the Id1^{low} population) appears in this model system to be compatible with the ability to transplant disease efficiently.

Id1^{high} cells generated tumors with high levels of Olig2 expression, which is consistent with acquisition of Olig2 in the Id1^{high} population being a critical factor in its tumorigenic potential, and previous studies have indeed shown an essential role for Olig2 in gliomagenesis (Ligon et al., 2007). While Id1^{high} cells were capable of generating tumors with Olig2 expression, Id1^{low} cells never reverted to an Id1-expressing state. Therefore, the lineage hierarchy of the normal neurogenic niche, which proceeds unidirectionally from stem cell to progenitor cell, was also maintained in our murine glioma models. We found no evidence for interconversion from an Id1^{low} progenitor state to an Id1^{high} stem-like state, although such dedifferentiation has been reported in in vitro systems (Kondo and Raff, 2000) and may occur under other oncogenic conditions. Thus, Id1^{low} cells need not dedifferentiate and acquire Id1 expression in order to transplant disease. Our results also suggest that Id1^{high} cells present in PDGF-driven gliomas likely arise from stem cell pools,

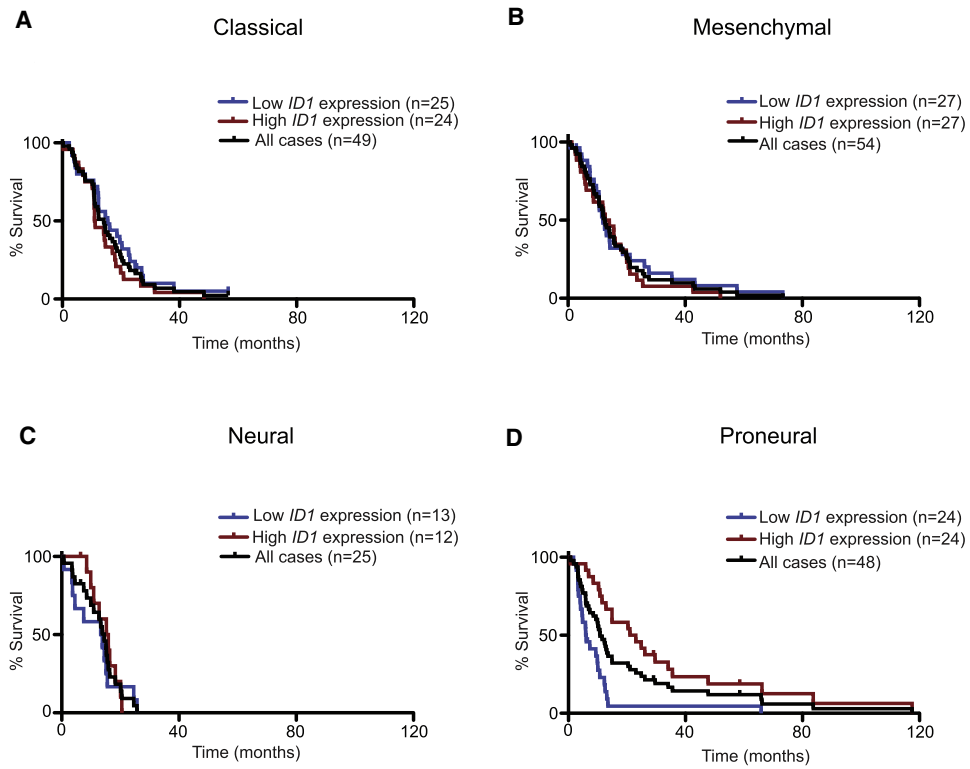

Figure 7. *ID1* Expression Levels Correlate with Survival of Human Patients within the Proneural Subclass of High-Grade Gliomas

Kaplan Meier analysis based on *ID1* expression using data from each of the four TCGA identified subtypes of primary GBM: (A) Classical ($p = 0.20$), (B) Mesenchymal ($p = 0.43$), (C) Neural ($p = 0.65$), and (D) Proneural. For the proneural subtype, the medium survival of patients with low and high Id1 expressing tumors are 6.015 months and 22.015 months, respectively ($p < 0.0001$).

rather than from expanding progenitor pools that revert to an $Id1^{high}$ state.

The Id1-expressing cells observed in tumors generated from $Id1^{low}$ cells were derived exclusively from the host, and Fomchenko et al. (2011) recently found significant roles for recruited cells in PDGF-driven murine gliomas. These cells were shown to aid in disease transplantation and had the capacity to become independent of the initiating oncogene (Fomchenko et al., 2011). We found that Id1 expression in the recruited population was not required for tumor growth, which was largely unaffected when $Id1^{low}$ cells were transplanted into an $Id1^{-/-}$ background. Our Id1-knockout studies further support the idea that Id1 expression and self-renewal capacity is not essential for tumor growth. If tumors were dependent upon self-renewal for their growth potential, we would expect that knockout of Id1, which significantly impacted tumorsphere formation, would have a greater impact on overall survival than observed. Our Olig2-knockdown studies lend further support to the notion that progenitor cell lineages may make greater contributions to tumor growth in PDGF-driven gliomas.

ID Genes in High-Grade Gliomas

We have isolated glioma cells that express high levels of Id1, and find that they represent a highly self-renewing population of tumor cells, allowing us to probe the role of self-renewal in glioma growth, rather than the role of *ID* genes in glioma biology generally. However, multiple *ID* genes are upregulated in high-grade gliomas and implicated in glioma pathogenesis (Vandeputte et al., 2002), and *ID* genes are known to have roles in tumor biology beyond self-renewal, including neoangiogenesis and regulation of cell-cycle (Perk et al., 2005). Recently, Anido et al. (2010) isolated a $CD44^{high}$ cell population from human patient derived glioma cells characterized by high levels of Id1 expression, TGF-ß-responsiveness and stem-like properties. These data are consistent with our results showing a role for Id1 in glioma cell self-renewal, and points to TGF-ß as a likely upstream regulator of Id1. While Id3 cosegregated with Id1 in our assays, Id2 and Id4 did not. It is likely that Id1/Id3 and Id2 and Id4 are expressed in different cell types and possess different functional roles depending on the specific tumorigenic context. While the effects of loss of Id1/3 on overall survival were modest in our model systems, it is possible that targeting additional Id proteins would yield a more dramatic effect, as this may impact both stem- and progenitor-like cell populations. In fact, recent studies indicate that combined loss of Id1, Id2, and Id3 impacts glioma cell self-renewal as well as proliferation, leading to a significant delay in tumor progression (A.I., unpublished observations). Our finding that multiple lineages are capable of transplanting disease suggests that targeting a single cell population alone may not yield optimal therapeutic effects in these tumor subtypes.

Relevance to Human Disease

This work raises a number of questions regarding the origin and propagation of human high-grade gliomas. We know that

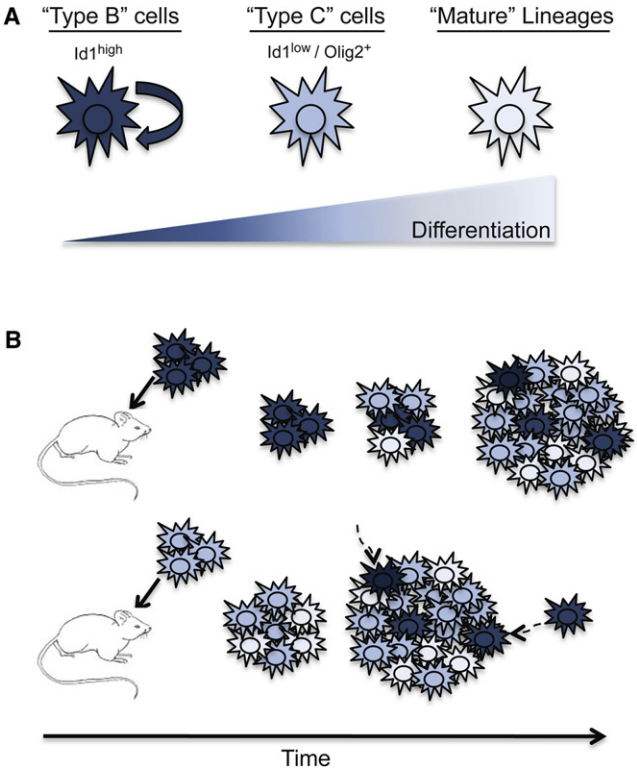

Figure 8. Proposed Model of High and Low Self-Renewing Lineages in Gliomagenesis

(A) Model depicting Id1^{high} cells, Id1^{low}/Olig2^{+} cells, and mature lineages.
(B) Comparison of Id1^{high} cells and Id1^{low}/Olig2^{+} cells in disease transplantation. Arrow represents recruitment of Id1-expressing cells to the tumor bulk.

multiple subclasses of human gliomas show a similar pattern of Id1 and Olig2 upregulation (Anido et al., 2010; Ligon et al., 2007; Vandeputte et al., 2002) and studies exploring at the effects of Olig2 knockdown in primary human glioma cells also show a significant delay in tumor development upon orthotopic transplantation (Mehta et al., 2011), consistent with our mouse knockdown experiments. Further, data from TCGA suggest that, within the Proneural subclass, high Id1 expression is associated with a better survival outcome. As gliomas are highly heterogeneous tumors that can be classified into multiple subtypes, further work will be required to determine the role of self-renewing, stem-like cells in tumors generated with other mutations and amplifications as well as the relative response of these different cell populations to radiation and chemotherapy. It is possible that stem-like and progenitor-like cells have different contributions to tumorigenesis depending on the oncogenic context, and a careful analysis of these cell populations in additional tumor subtypes will be important for determining the optimal cell populations for therapeutic targeting.

EXPERIMENTAL PROCEDURES

In Vivo Models

Nestin-tva; Arf$^{-/-}$ mice (Hambardzumyan et al., 2009), Id1^{VenusYFP} mice, Id1$^{flox/flox}$ mice (Nam and Benezra, 2009), and Id1$^{-/-}$ mice (Lyden et al., 1999) have been described. ubc-GFP mice were crossed with NOD-SCID mice to generate ubc-GFP;NOD-SCIDs. All mouse experiments were approved by MSKCC's Institutional Animal Care and Use Committee (IACUC).

Immunostaining

The following primary antibodies were used: Id1 (Biocheck), Id3 (Biocheck), Olig2 (Millipore), MAP2 (Millipore), GFAP (Millipore), Tuj1 (mouse, Millipore), Tuj1 (rabbit, Covance), O4 (Millipore), Nestin (BD Biosciences), phosphorylated histone H3 (H3P; Sigma), Cleaved Caspase 3 (Cell Signaling Technology), CD133 (Miltenyi Biotech), and GFP (Abcam).

Flow Cytometry

Cells were sorted for VenusYFP expression with PI exclusion at our FACS facility using a MoFlo cell sorter (Cytomation).

In Vitro Tumorsphere Assays

Tumors were papain digested (Worthington Biochemical), triturated and cells were plated for in vitro analysis in Neurocult Stem Cell Basal Media with Proliferation Supplements, 20 ng/ml EGF, 10 ng/ml FGF, and 2 μg/ml heparin (Stem Cell Technologies).

TCGA Kaplan-Meier Analysis

Id1 expression data were retrieved from the MSKCC cBio Cancer Genomics Portal (http://www.cbioportal.org/public-portal/). Patients were subdivided into high Id1 expression (top 50%) and low expression (bottom 50%) for analysis.

Statistics

Kaplan-Meier survival curves were generated with Prism software. All experiments were carried out in triplicate or greater. All p values are two-tailed and p values < 0.05 were considered significant. Data are shown as mean ± SD.

SUPPLEMENTAL INFORMATION

Supplemental Information includes six figures and Supplemental Experimental Procedures and can be found with this article online at doi:10.1016/j.ccr.2011.11.025.

ACKNOWLEDGMENTS

The authors thank members of the Benezra laboratory; E. Fomchenko, K. Pitter, and T. Ozawa for technical advice and reagents; The Laboratory of Comparative Pathology, Flow Cytometry Core Facility and Molecular Cytology Core Facility (MSKCC). Funding was provided through the Brain Tumor Center, MSKCC (L.E.B.), Ladies Auxiliary to the Veterans of Foreign Wars Postdoctoral Cancer Research Fellowship (L.E.B.), and the Kleberg Foundation (R.B.).

Received: June 28, 2011
Revised: October 20, 2011
Accepted: November 29, 2011
Published: January 17, 2012

REFERENCES

Alcantara Llaguno, S., Chen, J., Kwon, C.H., Jackson, E.L., Li, Y., Burns, D.K., Alvarez-Buylla, A., and Parada, L.F. (2009). Malignant astrocytomas originate from neural stem/progenitor cells in a somatic tumor suppressor mouse model. Cancer Cell *15*, 45–56.

Anido, J., Sáez-Borderías, A., Gonzàlez-Juncà, A., Rodón, L., Folch, G., Carmona, M.A., Prieto-Sánchez, R.M., Barba, I., Martínez-Sáez, E., Prudkin, L., et al. (2010). TGF-β Receptor Inhibitors Target the CD44(high)/Id1(high) Glioma-Initiating Cell Population in Human Glioblastoma. Cancer Cell *18*, 655–668.

Assanah, M., Lochhead, R., Ogden, A., Bruce, J., Goldman, J., and Canoll, P. (2006). Glial progenitors in adult white matter are driven to form

malignant gliomas by platelet-derived growth factor-expressing retroviruses. J. Neurosci. *26*, 6781–6790.

Beier, D., Hau, P., Proescholdt, M., Lohmeier, A., Wischhusen, J., Oefner, P.J., Aigner, L., Brawanski, A., Bogdahn, U., and Beier, C.P. (2007). CD133(+) and CD133(-) glioblastoma-derived cancer stem cells show differential growth characteristics and molecular profiles. Cancer Res. *67*, 4010–4015.

Brennan, C., Momota, H., Hambardzumyan, D., Ozawa, T., Tandon, A., Pedraza, A., and Holland, E. (2009). Glioblastoma subclasses can be defined by activity among signal transduction pathways and associated genomic alterations. PLoS ONE *4*, e7752.

Broadley, K.W., Hunn, M.K., Farrand, K.J., Price, K.M., Grasso, C., Miller, R.J., Hermans, I.F., and McConnell, M.J. (2011). Side population is not necessary or sufficient for a cancer stem cell phenotype in glioblastoma multiforme. Stem Cells *29*, 452–461.

Chen, R., Nishimura, M.C., Bumbaca, S.M., Kharbanda, S., Forrest, W.F., Kasman, I.M., Greve, J.M., Soriano, R.H., Gilmour, L.L., Rivers, C.S., et al. (2010). A hierarchy of self-renewing tumor-initiating cell types in glioblastoma. Cancer Cell *17*, 362–375.

Chow, L.M., Endersby, R., Zhu, X., Rankin, S., Qu, C., Zhang, J., Broniscer, A., Ellison, D.W., and Baker, S.J. (2011). Cooperativity within and among Pten, p53, and Rb pathways induces high-grade astrocytoma in adult brain. Cancer Cell *19*, 305–316.

Clément, V., Dutoit, V., Marino, D., Dietrich, P.Y., and Radovanovic, I. (2009). Limits of CD133 as a marker of glioma self-renewing cells. Int. J. Cancer *125*, 244–248.

Doetsch, F., García-Verdugo, J.M., and Alvarez-Buylla, A. (1997). Cellular composition and three-dimensional organization of the subventricular germinal zone in the adult mammalian brain. J. Neurosci. *17*, 5046–5061.

Fomchenko, E.I., Dougherty, J.D., Helmy, K.Y., Katz, A.M., Pietras, A., Brennan, C., Huse, J.T., Milosevic, A., and Holland, E.C. (2011). Recruited cells can become transformed and overtake PDGF-induced murine gliomas in vivo during tumor progression. PLoS ONE *6*, e20605.

Galli, R., Binda, E., Orfanelli, U., Cipelletti, B., Gritti, A., De Vitis, S., Fiocco, R., Foroni, C., Dimeco, F., and Vescovi, A. (2004). Isolation and characterization of tumorigenic, stem-like neural precursors from human glioblastoma. Cancer Res. *64*, 7011–7021.

Hambardzumyan, D., Amankulor, N.M., Helmy, K.Y., Becher, O.J., and Holland, E.C. (2009). Modeling Adult Gliomas Using RCAS/t-va Technology. Transl Oncol *2*, 89–95.

Hambardzumyan, D., Parada, L.F., Holland, E.C., and Charest, A. (2011). Genetic modeling of gliomas in mice: new tools to tackle old problems. Glia *59*, 1155–1168.

He, S., Nakada, D., and Morrison, S.J. (2009). Mechanisms of stem cell self-renewal. Annu. Rev. Cell Dev. Biol. *25*, 377–406.

Huse, J.T., Phillips, H.S., and Brennan, C.W. (2011). Molecular subclassification of diffuse gliomas: seeing order in the chaos. Glia *59*, 1190–1199.

Jackson, E.L., Garcia-Verdugo, J.M., Gil-Perotin, S., Roy, M., Quinones-Hinojosa, A., VandenBerg, S., and Alvarez-Buylla, A. (2006). PDGFR alpha-positive B cells are neural stem cells in the adult SVZ that form glioma-like growths in response to increased PDGF signaling. Neuron *51*, 187–199.

Kang, S.K., Park, J.B., and Cha, S.H. (2006). Multipotent, dedifferentiated cancer stem-like cells from brain gliomas. Stem Cells Dev. *15*, 423–435.

Kondo, T., and Raff, M. (2000). Oligodendrocyte precursor cells reprogrammed to become multipotent CNS stem cells. Science *289*, 1754–1757.

Ligon, K.L., Alberta, J.A., Kho, A.T., Weiss, J., Kwaan, M.R., Nutt, C.L., Louis, D.N., Stiles, C.D., and Rowitch, D.H. (2004). The oligodendroglial lineage marker OLIG2 is universally expressed in diffuse gliomas. J. Neuropathol. Exp. Neurol. *63*, 499–509.

Ligon, K.L., Huillard, E., Mehta, S., Kesari, S., Liu, H., Alberta, J.A., Bachoo, R.M., Kane, M., Louis, D.N., Depinho, R.A., et al. (2007). Olig2-regulated lineage-restricted pathway controls replication competence in neural stem cells and malignant glioma. Neuron *53*, 503–517.

Lindberg, N., Kastemar, M., Olofsson, T., Smits, A., and Uhrbom, L. (2009). Oligodendrocyte progenitor cells can act as cell of origin for experimental glioma. Oncogene *28*, 2266–2275.

Liu, C., Sage, J.C., Miller, M.R., Verhaak, R.G., Hippenmeyer, S., Vogel, H., Foreman, O., Bronson, R.T., Nishiyama, A., Luo, L., and Zong, H. (2011). Mosaic analysis with double markers reveals tumor cell of origin in glioma. Cell *146*, 209–221.

Lyden, D., Young, A.Z., Zagzag, D., Yan, W., Gerald, W., O'Reilly, R., Bader, B.L., Hynes, R.O., Zhuang, Y., Manova, K., and Benezra, R. (1999). Id1 and Id3 are required for neurogenesis, angiogenesis and vascularization of tumour xenografts. Nature *401*, 670–677.

Mehta, S., Huillard, E., Kesari, S., Maire, C.L., Golebiowski, D., Harrington, E.P., Alberta, J.A., Kane, M.F., Theisen, M., Ligon, K.L., et al. (2011). The central nervous system-restricted transcription factor Olig2 opposes p53 responses to genotoxic damage in neural progenitors and malignant glioma. Cancer Cell *19*, 359–371.

Menn, B., Garcia-Verdugo, J.M., Yaschine, C., Gonzalez-Perez, O., Rowitch, D., and Alvarez-Buylla, A. (2006). Origin of oligodendrocytes in the subventricular zone of the adult brain. J. Neurosci. *26*, 7907–7918.

Nam, H.S., and Benezra, R. (2009). High levels of Id1 expression define B1 type adult neural stem cells. Cell Stem Cell *5*, 515–526.

Network, T.C.G.A.T.R.; Cancer Genome Atlas Research Network. (2008). Comprehensive genomic characterization defines human glioblastoma genes and core pathways. Nature *455*, 1061–1068.

Pastrana, E., Silva-Vargas, V., and Doetsch, F. (2011). Eyes wide open: a critical review of sphere-formation as an assay for stem cells. Cell Stem Cell *8*, 486–498.

Perk, J., Iavarone, A., and Benezra, R. (2005). Id family of helix-loop-helix proteins in cancer. Nat. Rev. Cancer *5*, 603–614.

Persson, A.I., Petritsch, C., Swartling, F.J., Itsara, M., Sim, F.J., Auvergne, R., Goldenberg, D.D., Vandenberg, S.R., Nguyen, K.N., Yakovenko, S., et al. (2010). Non-stem cell origin for oligodendroglioma. Cancer Cell *18*, 669–682.

Prestegarden, L., and Enger, P.O. (2010). Cancer stem cells in the central nervous system—a critical review. Cancer Res. *70*, 8255–8258.

Romero-Lanman, E.E., Pavlovic, S., Amlani, B., Chin, Y., and Benezra, R. (2011). Id1 maintains embryonic stem cell self-renewal by up-regulation of Nanog and repression of Brachyury expression. Stem Cells Dev. 10.1089/scd.2011.0428.

Singh, S.K., Clarke, I.D., Terasaki, M., Bonn, V.E., Hawkins, C., Squire, J., and Dirks, P.B. (2003). Identification of a cancer stem cell in human brain tumors. Cancer Res. *63*, 5821–5828.

Singh, S.K., Hawkins, C., Clarke, I.D., Squire, J.A., Bayani, J., Hide, T., Henkelman, R.M., Cusimano, M.D., and Dirks, P.B. (2004). Identification of human brain tumour initiating cells. Nature *432*, 396–401.

Stiles, C.D., and Rowitch, D.H. (2008). Glioma stem cells: a midterm exam. Neuron *58*, 832–846.

Sun, Y., Meijer, D.H., Alberta, J.A., Mehta, S., Kane, M.F., Tien, A.C., Fu, H., Petryniak, M.A., Potter, G.B., Liu, Z., et al. (2011). Phosphorylation state of Olig2 regulates proliferation of neural progenitors. Neuron *69*, 906–917.

Terzis, A.J., Niclou, S.P., Rajcevic, U., Danzeisen, C., and Bjerkvig, R. (2006). Cell therapies for glioblastoma. Expert Opin. Biol. Ther. *6*, 739–749.

Uhrbom, L., and Holland, E.C. (2001). Modeling gliomagenesis with somatic cell gene transfer using retroviral vectors. J. Neurooncol. *53*, 297–305.

Uhrbom, L., Kastemar, M., Johansson, F.K., Westermark, B., and Holland, E.C. (2005). Cell type-specific tumor suppression by Ink4a and Arf in Kras-induced mouse gliomagenesis. Cancer Res. *65*, 2065–2069.

Vandeputte, D.A., Troost, D., Leenstra, S., Ijlst-Keizers, H., Ramkema, M., Bosch, D.A., Baas, F., Das, N.K., and Aronica, E. (2002). Expression and distribution of id helix-loop-helix proteins in human astrocytic tumors. Glia *38*, 329–338.

Verhaak, R.G., Hoadley, K.A., Purdom, E., Wang, V., Qi, Y., Wilkerson, M.D., Miller, C.R., Ding, L., Golub, T., Mesirov, J.P., et al; Cancer Genome Atlas Research Network. (2010). Integrated genomic analysis identifies clinically

relevant subtypes of glioblastoma characterized by abnormalities in PDGFRA, IDH1, EGFR, and NF1. Cancer Cell *17*, 98–110.

Wang, J., Sakariassen, P.O., Tsinkalovsky, O., Immervoll, H., Bøe, S.O., Svendsen, A., Prestegarden, L., Røsland, G., Thorsen, F., Stuhr, L., et al. (2008). CD133 negative glioma cells form tumors in nude rats and give rise to CD133 positive cells. Int. J. Cancer *122*, 761–768.

Yang, Z.J., Ellis, T., Markant, S.L., Read, T.A., Kessler, J.D., Bourboulas, M., Schüller, U., Machold, R., Fishell, G., Rowitch, D.H., et al. (2008). Medulloblastoma can be initiated by deletion of Patched in lineage-restricted progenitors or stem cells. Cancer Cell *14*, 135–145.

Ying, Q.L., Nichols, J., Chambers, I., and Smith, A. (2003). BMP induction of Id proteins suppresses differentiation and sustains embryonic stem cell self-renewal in collaboration with STAT3. Cell *115*, 281–292.